

Thesis

$S = 1$ Antiferromagnetic Heisenberg Chain
in a Magnetic Field

(和訳: 磁場中の $S = 1$ 反強磁性ハイゼンベルグ鎖)

Tōru Sakai

坂井 徹



Thesis

**$S = 1$ Antiferromagnetic Heisenberg Chain
in a Magnetic Field**

Tōru Sakai

Department of Material Science

Faculty of Science

Himeji Institute of Technology

Kamigori-cho, Ako-gun, Hyogo 678-12

Abstract

The $S = 1$ antiferromagnetic Heisenberg chain in a magnetic field along the z -axis at $T = 0$ is studied by numerical diagonalizations up to $N = 16$ and an analysis of the finite size scaling. The system has two phase transitions at $H_{c1}(= \Delta)$ and $H_{c2}(= 4)$, where Δ is the Haldane gap; the ground state has $m = 0$ for $H < H_{c1}$ and $m = 1$ for $H > H_{c2}$, where m is the magnetization. We give the magnetization curve in the thermodynamic limit, check that the system obeys the conformal field theory with the central charge $c = 1$ in a magnetic state ($0 < m < 1$). We investigate the asymptotic form of the transverse and parallel spin correlations and give the exponents η and η^z , defined by $\langle S_0^x S_r^x \rangle \simeq (-1)^r r^{-\eta}$ and $\langle S_0^z S_r^z \rangle - m^2 \simeq \cos(2k_F r) r^{-\eta^z}$. We determine $\eta = 1/2$ and $\eta^z = 2$ at $m = 0$ and 1. In addition, we check the relation $\eta\eta^z = 1$, which is consistent with the Luttinger liquid concept. In terms of the concept, the anomalies of magnetization at $m = 0$ and 1 are discussed. It is found that if the system is quasi-one-dimensional, even small interchain interactions can make canting Néel order, within a mean field approximation for interchain interactions. It is consistent with a recent NMR measurement for NENP at low temperature.

Contents

Chapter 1. Introduction	...3
§1. 1 Antiferromagnetic Heisenberg Chain	...3
§1. 2 Haldane Conjecture	...5
§1. 3 Theoretical supports	...7
§1. 3. 1 Numerical Approaches	...7
§1. 3. 2 Analytical Approaches	...8
§1. 4 Quasi-One-Dimensional Case	...10
§1. 5 Behaviors in a Magnetic Field	...11
Chapter 2. Magnetization Curve	...16
§2. 1 Numerical Calculation and Notation	...16
§2. 2 Size Dependence of Energy	...19
§2. 3 Extrapolated Results	...21
§2. 3. 1 Magnetization	...21
§2. 3. 2 Field Derivative	...24
§2. 4 Anomalies at H_{c1} and H_{c2}	...25
Chapter 3. Spin Correlation	...38
§3. 1 Numerical Calculation and Notation	...38
§3. 2 Prediction from Conformal Invariance	...40
§3. 3 Central Charge	...42
§3. 4 Spin Correlation Exponents	...44

§3. 4. 1 Transverse Spin Correlation	...44
§3. 4. 2 Parallel Spin Correlation	...46
§3. 5 Luttinger Liquid Concept	...48
§3. 6 Anomalies of Magnetization Curve	...51
Chapter 4. Quasi-One-Dimensional Case	...60
§4. 1 Mean Field Approximation for Interchain Interaction	...60
§4. 2 Staggered Susceptibility of One-Dimensional System	...63
§4. 3 Consistency with Experiment	...68
Chapter 5. Summery	...75

Chapter 1. Introduction

§1. 1 Antiferromagnetic Heisenberg Chain

The Antiferromagnetic Heisenberg model has attracted great interest for many years. It is defined by the Hamiltonian

$$\mathcal{H} = \sum_{\langle i,j \rangle} \mathbf{S}_i \cdot \mathbf{S}_j, \quad (1-1)$$

where $\sum_{\langle i,j \rangle}$ means the sum for all the nearest neighbor pairs, and the spin operators \mathbf{S}_i obey the commutation relation

$$[S_i^a, S_j^b] = i\delta_{ij}\epsilon^{abc}S_i^c, \quad (1-2)$$

and the constraint $\mathbf{S}_i \cdot \mathbf{S}_i = S(S+1)$. The value of S is allowed to be $1/2, 1, 3/2, 2, \dots$. The model describes the magnetic properties of many antiferromagnetic insulators.

It has been exactly shown that the model has no long-range Néel order at finite temperature for one and two dimensions.¹ Only the ground state has Néel order for two dimensions, which is supported by a rigorous proof^{2,3} at least for $S \geq 1$, and many theories⁴⁻⁸ show the existence of the order even for $S = 1/2$. But one-dimensional model has no Néel order even at $T = 0$, because the quantum fluctuation is very large. It has not been shown exactly yet. The exact ground state has been derived from the Bethe ansatz method⁹ only

for $S = 1/2$. The model has been shown to have a gapless and linear dispersion of the spin wave excitation,¹⁰ and the spin correlation decaying algebraically as

$$\langle S_0^z S_r^z \rangle \simeq (-1)^r \frac{1}{r} \quad (r \rightarrow \infty), \quad (1-3)$$

in the ground state.¹¹ In this case Néel order does not exist but the correlation length is infinite at $T = 0$, which means that $T = 0$ is a critical point. It had been thought that these behaviors for $S = 1/2$ are common to all antiferromagnetic Heisenberg chains even for higher spins, until Haldane proposed a conjecture mentioned in the next section.

§1. 2 Haldane Conjecture

Haldane predicted¹² that the one-dimensional Heisenberg antiferromagnet has an energy gap in the excitation spectrum for integral S , but not for half-integral S . The gap for integral S is called the "Haldane gap". This prediction is based on mapping^{12,13} the original model to the non-linear σ -model in 1 + 1 space-time dimensions which has an energy gap,¹⁴⁻¹⁷ taking a semiclassical and continuous limit after describing the spin operators by the operators

$$\mathbf{n}_{2i} = \frac{\mathbf{S}_{2i+1} - \mathbf{S}_{2i}}{2S}, \quad \mathbf{l}_{2i} = \frac{\mathbf{S}_{2i+1} + \mathbf{S}_{2i}}{2a}, \quad (1-4)$$

where a is the lattice constant. This mapping gives the model described by the Lagrangian

$$\mathcal{L} = \frac{1}{2g} \partial_\mu \mathbf{n} \cdot \partial^\mu \mathbf{n} + \frac{\theta}{8\pi} \epsilon^{\mu\nu} \mathbf{n} \cdot (\partial_\mu \mathbf{n} \times \partial_\nu \mathbf{n}), \quad (1-5)$$

and the constraint

$$\mathbf{n}^2 = 1, \quad (1-6)$$

where $g = 2/S$ and $\theta = 2\pi S$. The second term is the topological term which is of no effect for integral S . Haldane suggested that the existence of the topological term leads to the different properties between integral- S and half-integral- S cases, on the quantization of the instanton solution for the non-linear σ -model.

The prediction also suggested that the spin correlation decays exponentially with a finite correlation length for integral S , but the

one decays algebraically for half-integral S . Thus the properties of the ground state and the excitation spectrum for half-integral S are qualitatively the same as for $S = 1/2$, but the ones for integral S are essentially different. If the prediction is true, the system is not critical even at $T = 0$ for integral S . It means that the quantum fluctuation which breaks the Néel order is larger for integral S . The fact that the qualitative property depends on the value of S is a topological effect characteristic of the one-dimensional system.

§1. 3 Theoretical Supports

§1. 3. 1 Numerical Approaches

The Haldane conjecture has been supported by many numerical calculations for $S = 1$. At first the phenomenological renormalization¹⁸ based on numerical diagonalization up to $N = 12$ yielded evidence of the fact that the energy gap closes at two points as the anisotropy of the coupling constant λ defined by

$$H = \sum_j (S_j^x S_{j+1}^x + S_j^y S_{j+1}^y + \lambda S_j^z S_{j+1}^z), \quad (1-7)$$

varies. Recent calculations¹⁹ for larger-size systems showed that the two transitions are Kosterlitz-Thouless-type ($\lambda_c = -0.01 \pm 0.03$) and two-dimensional-Ising-type ($\lambda_c = 1.188 \pm 0.007$), as Haldane predicted. The value of the energy gap in the thermodynamic limit was estimated to be 0.41 by a Monte Carlo simulation²⁰ up to $N = 32$ and 0.411 ± 0.001 by a numerical diagonalization²¹ up to $N = 16$. In addition the difference of the excitation energy spectrum²² for $S = 1/2$ and $S = 1$, and the asymptotic form of the spin correlation decaying exponentially²³ were checked by the projector Monte Carlo methods. The correlation length estimated to be 5.5 ± 2 from the excitation spectrum,²⁴ 6.3 from the correlation function,²³ and 8.3 from a quantum-transfer-matrix method.²⁵

§1. 3. 2 Analytical Approaches

Other than Haldane's original work, some analytical approaches supported the conjecture. A method²⁶ representing a spin- S operator as the sum of $2S$ spin-1/2 operators, and taking a weak-coupling and continuum limit, led to the difference of the spin correlation between integral S and half-integral S .

An exactly solvable model for $S = 1$ was found.²⁷ It is given by the Hamiltonian

$$\mathcal{H} = \sum_j \mathbf{S}_j \cdot \mathbf{S}_{j+1} + \frac{1}{3} \sum_j (\mathbf{S}_j \cdot \mathbf{S}_{j+1})^2, \quad (1-8)$$

which has the same symmetry as the Heisenberg Hamiltonian. It was exactly shown that the model has an energy gap and the spin correlation decays exponentially in the ground state.

The original Hamiltonian for $S = 1$ was studied in a reduced Hilbert space²⁸ where the two spins at the left and right of a spin-0 ($S^z = 0$) site (or a sequence of spin-0 sites) should be antiparallel. A typical example of a state within this restricted space could have the form

$$\cdots \uparrow \downarrow 0 \uparrow 00 \downarrow \uparrow \downarrow 0 \uparrow \cdots.$$

The model is equivalent to the transverse Ising model in the space and it is found that the two-dimensional-Ising-type transition occurs as an anisotropy of the coupling constant varies. This approximation

is good to study the low-temperature behavior of the original model. In fact the excitation spectrum given by this method agrees with the one by the Monte Carlo calculation²² within the statistical errors for the region near $k = 0$ or π . In addition the ground state of the solvable model (1 - 8) was shown to be in the reduced Hilbert space.^{27,29}

§1. 4 Quasi-One-Dimensional Case

Some experimental studies³⁰⁻³³ have also given the evidence of the Haldane gap for $\text{Ni}(\text{C}_2\text{H}_8\text{N}_2)_2\text{NO}_2(\text{ClO}_4)$, abbreviated NENP, which is an $S = 1$ quasi-one-dimensional antiferromagnet. Although most real quasi-one-dimensional antiferromagnets have Néel order due to interchain interactions at low temperature, NENP has no Néel order at least down to 1.2K(Ref. 30). It was expected that, if interchain interactions are small enough, the system has no Néel order even at $T = 0$. This has been supported by some theoretical studies, which are a perturbative approach³⁴, a field theoretical analysis³⁵, a mean field approximation for interchain couplings³⁶, and a rigorous proof in the reduced Hilbert space³⁷. Using mean field approximation for interchain interactions, it has been shown³⁸ that NENP has no Néel order even at $T = 0$. Thus the Haldane gap can exist also in a quasi-one-dimensional system such as NENP, which is intrinsically three-dimensional.

§1. 5 Behaviors in a Magnetic Field

High-field magnetization measurements^{32,33} have also indicated the evidence of the Haldane gap for NENP. According to those experiments, a transition from the nonmagnetic to the magnetic state at H_{c1} . Those support the existence of an energy gap between the ground state with $\sum_j S_j^z = 0$ and the first excited states with $\sum_j S_j^z = \pm 1$. It is also noted that the curve of the field derivative $\frac{dm}{dH}$ in an experiment³³ has an anomalous behavior at H_{c1} .

Recently it has been reported that an NMR measurement³⁸ indicated the strong antiferromagnetic correlation for the magnetic state of NENP in a magnetic field. Then it is expected that the canted Néel order, that is, the state which has both ferromagnetic order along z -axis($\parallel H$) and staggered magnetization in xy -plane($\perp H$), exists at sufficiently low temperature.

The magnetization curve for $S = 1$ was given by a numerical diagonalization⁴⁰ up to $N = 14$, but the result was not extrapolated to the thermodynamic limit and it did not give any singularities near the critical field.

In this thesis we study a one-dimensional $S = 1$ Heisenberg antiferromagnet in a magnetic field H at $T = 0$ by numerical diagonalizations up to $N = 16$ and the finite size scaling. In chapter 2 we give the magnetization curve in the thermodynamic limit and suggest

the existence of an anomaly at H_{c1} . In chapter 3 we show that the transverse and parallel spin correlations decay algebraically for the magnetic state and estimated the exponents of the power-law decay applying the conformal field theory⁴¹ to the excitation energy spectrum of finite systems. Then we determine the forms of anomalies in the magnetization curve using the consistency with the Luttinger liquid theory.⁴² In chapter 4 we study the quasi-one-dimensional case using a mean field approximation for interchain interactions, and conclude that a transition from disorder to canted Néel order exists at H_{c1} .

References

- ¹ N. D. Mermin and H. Wagner, Phys. Rev. Lett. **17**, 1133 (1966).
- ² E. J. Neves and J. F. Perez, Phys. Lett. **114A**, 331 (1986).
- ³ F. J. Dyson, E. H. Lieb and B. Simon, J. Stat. Phys. **18**, 335 (1978).
- ⁴ J. D. Reger and A. P. Young, Phys. Rev. **B37**, 5978 (1988).
- ⁵ J. Oitmaa and D. D. Betts, Can. J. Phys. **56**, 897 (1978).
- ⁶ D. A. Huse, Phys. Rev. **B37**, 2380 (1988).
- ⁷ P. W. Anderson, Phys. Rev. **86**, 694 (1952).
- ⁸ R. Kubo, Phys. Rev. **87**, 568 (1952).
- ⁹ H. A. Bethe, Z. Phys. **71**, 205 (1931) ; L. Hulthén, Arkiv Mat. Astron. Fysik **26A**, 1 (1938).
- ¹⁰ J. des Cloizeaux and J. J. Pearson, Phys. Rev. **128**, 2131 (1962).
- ¹¹ A. Luther and I. Peschel, Phys. Rev. **B12**, (1975) 3908.
- ¹² F. D. M. Haldane, Phys. Lett. **93A**, 464 (1983); Phys. Rev. Lett. **50**, 1153 (1983).
- ¹³ I. Affleck, Phys. Rev. Lett. **56**, 408 (1986).
- ¹⁴ A. A. Belavin and A. M. Polyakov, JETP Lett. **22**, 245 (1975).
- ¹⁵ E. Brézin and J. Zinn-Justin, Phys. Rev. **B14**, 3210 (1976).
- ¹⁶ V. A. Fateev, I. V. Frolov, and A. S. Schwartz, Nucl. Phys. **B154**, 1 (1979).

- ¹⁷ B. Berg and M. Lüscher, *Commun. Math. Phys.* **69**, 57 (1979).
- ¹⁸ R. Botet and R. Jullien, *Phys. Rev.* **B27**, 613 (1983); R. Botet, R. Jullien, and M. Kolb, *ibid.* **28**, 3914 (1983); M. Kolb, R. Botet, and R. Jullien, *J. Phys.* **A16**, L673(1983).
- ¹⁹ T. Sakai and M. Takahashi, *J. Phys. Soc. Jpn.* **59**, 2688 (1990).
- ²⁰ M. P. Nightingale and H. W. Blöte, *Phys. Rev.* **B33**, 659 (1986).
- ²¹ T. Sakai and M. Takahashi, *Phys. Rev.* **B42**, 1090 (1990).
- ²² M. Takahashi, *Phys. Rev. Lett.* **62**, 2313 (1989).
- ²³ K. Nomura, *Phys. Rev.* **B40**, 2421 (1989).
- ²⁴ M. Takahashi, *Phys. Rev.* **B38**, 5188 (1988).
- ²⁵ K. Kubo and S. Takada, *J. Phys. Soc. Jpn.* **55**, 438 (1986).
- ²⁶ H. J. Schulz, *Phys. Rev.* **B34**, 6372 (1986).
- ²⁷ I. Affleck, T. Kennedy, E. H. Lieb, and H. Tasaki, *Phys. Rev. Lett.* **59**, 799 (1987); *Commun. Math. Phys.* **115**, 477 (1988).
- ²⁸ G. Gómez-Santos, *Phys. Rev. Lett.* **63**, 790 (1989).
- ²⁹ H. Tasaki, *Phys. Rev. Lett.* **66**, 798 (1991).
- ³⁰ J. P. Renard, M. Verdaguer, L. P. Regnault, W. A. C. Erkelens, J. Rossat-Mignod, and W. G. Stirling, *Europhys. Lett.* **3**, 945 (1987).
- ³¹ J. P. Renard, M. Verdaguer, L. P. Regnault, W. A. C. Erkelens, J. Rossat-Mignod, J. Ribas, W. G. Stirling, and C. Vettier, *J.*

- Appl. Phys. **63**, 3538 (1988).
- ³² K. Katsumata, H. Hori, T. Takeuchi, M. Date, A. Yamagishi, and J. P. Renard, Phys. Rev. Lett. **63**, 86 (1989).
- ³³ Y. Ajiro, T. Goto, H. Kikuchi, T. Sakakibara, and T. Inami, Phys. Rev. Lett. **63**, 1424 (1989).
- ³⁴ Yu. A. Kosevich and A. V. Chubukov, Zh. Eksp. Theor. Fiz. **91**, 1105 (1986) [Sov. Phys. JETP **64**, 654 (1987)].
- ³⁵ I. Affleck, Phys. Rev. Lett. **62**, 474 (1989).
- ³⁶ T. Sakai and M. Takahashi, J. Phys. Soc. Jpn. **58**, 3131 (1989).
- ³⁷ H. Tasaki, Phys. Rev. Lett. **64**, 2066 (1990).
- ³⁸ T. Sakai and M. Takahashi, Phys. Rev. **B42**, 4537 (1990).
- ³⁹ M. Chiba, Y. Ajiro, H. Kikuchi, T. Kubo, and T. Morimoto, Phys. Rev. **B44**, 2838 (1991).
- ⁴⁰ J. B. Parkinson and J. C. Bonner, Phys. Rev. **B32**, 4703 (1985).
- ⁴¹ J. L. Cardy, in *Phase Transitions and Critical Phenomena*, edited by C. Domb and D. L. Lebowitz (Academic, London, 1987), Vol. 11, Chap. 2, p. 55.
- ⁴² F. D. M. Haldane, Phys. Rev. Lett. **45**, 1358 (1980); Phys. Lett. **81A**, 153 (1981); J. Phys. **C14**, 2585 (1981).

Chapter 2. Magnetization Curve

§2. 1 Numerical Calculation and Notation

We consider the magnetization process of the $S = 1$ one-dimensional antiferromagnetic Heisenberg model at $T = 0$ (Ref. 1). The Hamiltonian is

$$\begin{aligned}\mathcal{H} &= \mathcal{H}_0 + \mathcal{H}_1, \\ \mathcal{H}_0 &= \sum_j \mathbf{S}_j \cdot \mathbf{S}_{j+1}, \quad \mathcal{H}_1 = -H \sum_j S_j^z.\end{aligned}\tag{2-1}$$

We use the unit such as $g\mu_B = 1$, where g is the g -factor and μ_B is the Bohr magneton. NENP has the anisotropic term $D \sum_j S_j^z{}^2 + E \sum_j (S_j^x{}^2 - S_j^y{}^2)$. For simplicity we neglect this term. Since the commutation relation $[\sum_j S_j^z, \mathcal{H}_0] = 0$ is satisfied, \mathcal{H}_0 can be diagonalized within each subspace labeled by M independently, where M is the eigenvalue of $\sum_j S_j^z$. The role of \mathcal{H}_1 is only to shift each energy of \mathcal{H}_0 by $-HM$. We define $E(N, M)$ as the lowest energy of \mathcal{H}_0 in the subspace where $\sum_j S_j^z = M$, for an N -site system. We calculate $E(N, M)$ ($M = 0, 1, 2, \dots, N$) under the periodic boundary condition for even-site systems up to $N = 16$, using the Lanczos algorithm. The results are shown in Table 2-1. In this chapter, using those data, we give the magnetization curve in the thermodynamic limit. We define the magnetization m as $m \equiv M/N$. The numerical results up to $N = 16$ suggest that $E(N, M) - E(N, M-1)$ increases

with M monotonously. Thus the magnetization curve of the finite- N system at $T = 0$ is given by

$$m = \frac{M}{N} : M = \max\{M | E(N, M) - E(N, M - 1) < H\}, \quad (2-2)$$

which gives an N -step curve. So far the magnetization curve of a bulk system based on numerical calculation has been given only by connecting the middle points of the steps.² But we give the extrapolated magnetization curve for $N \rightarrow \infty$ at least for some points.

We define two critical fields; the ground state has $M = 0$ for $H < H_{c1}$, and $M = N$ for $H > H_{c2}$. The Haldane gap, which is defined as Δ , is the energy gap between the ground state and the triplet of the first excited states for \mathcal{H}_0 . These first excited states are the lowest-energy states in the subspaces where $M = \pm 1$ respectively and the second-lowest-energy state in the subspace where $M = 0$ (Ref. 3). Thus we get $\Delta = \lim_{N \rightarrow \infty} [E(N, 1) - E(N, 0)]$. At $H = E(N, 1) - E(N, 0)$, the ground state of the Hamiltonian (2-1) changes from non-magnetic to magnetic for an N -site system. Therefore $H_{c1} = \Delta$. We assumed that continuous spectrum corresponding to magnetized states exists above the gap. In addition, since the ground state of (2-1) has saturated magnetization for $H > E(N, N) - E(N, N - 1)$, we get $H_{c2} = \lim_{N \rightarrow \infty} [E(N, N) - E(N, N - 1)]$. The lowest-energy state in the subspace where $M = N - 1$ is exactly given by $N^{-1/2} \sum_{r=0}^{N-1} (-1)^r |\cdots 11011 \cdots\rangle_r$, where $|\cdots 11011 \cdots\rangle_r$ is the

state with $S_r^z = 0$ and $S_j^z = 1$ ($j \neq r$). The state has the energy $E(N, N-1) = N-4$, and $E(N, N) - E(N, N-1) = 4$ is independent of N . Thus the critical field H_{c2} is given by $H_{c2} = 4$.

§2. 2 Size Dependence of Energy

It is well known that the conformal field theory⁴ is a powerful method for one-dimensional quantum systems. It predicts that if the lowest-energy state is massless, the size-dependence of the energy per site has the form⁵

$$\frac{1}{N}E(N, M) \sim \epsilon(m) + A(m)\frac{1}{N^2} \quad (N \rightarrow \infty), \quad (2-3)$$

where $\epsilon(m)$ is the lowest energy per site in the thermodynamic limit. The second term represents the finite-size correction. It is noted that we must change N with $m = M/N$ fixed. Plots of $E(N, M)/N$ versus $1/N^2$ for $m = 0, 1/4, 1/2$, and $3/4$ are shown in Fig. 2-1. The plot is almost linear for $m \neq 0$, but the value for $m = 0$ converges faster than $1/N^2$. It suggests that the lowest-energy state is massless for $m \neq 0$, while massive only for $m = 0$. Thus we assume that the relation (2-3) is satisfied for $0 < m < 1$. In order to estimate $\epsilon(m)$, we extrapolate from the largest- and next-largest-size values of $E(N, M)/N$ by the form (2-3). For example, we use $E(16, 4)$ and $E(12, 3)$ to determine $\epsilon(1/4) = -1.1823 \pm 0.0002$. We estimate the error by the difference from the result extrapolated from the next- and next-next-largest-size data, which are $E(12, 3)$ and $E(8, 2)$ in the example. We can estimate $\epsilon(m)$ by this extrapolation, for $m = 1/8, 1/6, 1/4, 1/3, 5/8, 1/2, 3/8, 2/3, 3/4, 5/6$, and $7/8$. The error due to extrapolation is smaller than 0.01% for $m = 1/4$,

1/2, and 3/4. The error cannot be estimated for other values of m , because only two points can be used for extrapolation, for example, we can use only $N=8$ and 16 for $m=1/8$. But we think that these estimations are also sufficiently accurate to plot in the figure. In fact the difference between the estimation of $\epsilon(1/2)$ extrapolated from $E(14,7)$ and $E(16,8)$, and the one extrapolated from $E(6,3)$ and $E(12,6)$, is about 0.03%. Thus we think that estimations even from only two points are as accurate as it, because the size dependence of $E(N,M)$ does not have a drastic change when m changes in the region $0 < m < 1$, where the system is still massless. Estimated values of $\epsilon(m)$ are plotted in Fig. 2-2, where the value of $\epsilon(0)$ we use is the result of Vanden Broeck and Schwartz (VBS) method⁶ by Betsuyaku⁷.

§2. 3 Extrapolated Results

§2. 3. 1 Magnetization

Minimizing the total energy of the system $(2-1) \epsilon_{\text{tot}} = \epsilon(m) - Hm$, it is found that the magnetization curve at $T = 0$ is derived from

$$\epsilon'(m) = H, \quad (2-4)$$

in the thermodynamic limit. Now we assume that $\epsilon(m)$ and $A(m)$ are analytic for $0 < m < 1$. In this region, we use the form (2-3) to get the size-dependence of the spin-excitation gap, which is

$$E(N, M+1) - E(N, M) \sim \epsilon'(m) + \frac{1}{2}\epsilon''(m)\frac{1}{N} + O\left(\frac{1}{N^2}\right), \quad (2-5)$$

$$E(N, M) - E(N, M-1) \sim \epsilon'(m) - \frac{1}{2}\epsilon''(m)\frac{1}{N} + O\left(\frac{1}{N^2}\right). \quad (2-6)$$

The fact that the dominant finite-size correction of the gap is proportional to $1/N$ has been also derived directly from the conformal invariance (see the next chapter). In order to estimate $\epsilon'(m)$, we plot $E(N, M+1) - E(N, M)$ and $E(N, M) - E(N, M-1)$ versus $1/N$ in Fig. 2-3. Those curves are almost linear at least for $m = 1/4, 1/2$, and $3/4$. We use the largest- and next-largest-size data of $E(N, M+1) - E(N, M)$ to determine $\epsilon'(m)$ by the first and second terms of (2-5), and do the same treatment using $E(N, M) - E(N, M-1)$ and the form (2-6). The two results of $\epsilon'(m)$ coincide with each

other with difference less than 1% for $m \geq 1/4$. Only for $1/6$ and $1/8$, the difference is a few percent. Thus we regard the average of the two results based on (2-5) and (2-6) as the extrapolated value of $\epsilon(m)$, and the difference between the two as the error due to extrapolation. Now we consider the case of $m = 0$. It is found that $E(N, 1) - E(N, 0)$ converges faster than $1/N$, as shown by points connected by the dashed curve in Fig. 2-3. Even if we extrapolate it linearly to $1/N$, the result would be finite (~ 0.32). This is also the evidence of the Haldane gap. Here we estimate the gap Δ by applying Shanks' transformation⁸ to the sequence $\Delta(N) \equiv E(N, 1) - E(N, 0)$ up to $N = 16$. The transformation is one of techniques for accelerating the convergence of a sequence $\{P_n\}$ to its limit P_∞ , when $\{P_n\}$ satisfies

$$P_n = P_\infty + O(\epsilon^{-cn}), \quad n \rightarrow \infty, \quad (2-7)$$

where c is a constant⁹. The asymptotic form (2-7) is characteristic of data from a finite lattice when the system is not critical even at the thermodynamic limit. The algorithm of applying this transformation to a sequence $\{P_n\}$ is given by

$$P'_n = \frac{P_{n-1}P_{n+1} - P_n^2}{P_{n-1} + P_{n+1} - 2P_n}. \quad (2-8)$$

If $\{P_n\}$ is exactly of the form (2-8), then P'_n is exactly P_∞ , otherwise P'_n approaches P_∞ more rapidly than P_n . Since three data (P_{n-1} ,

P_n , and P_{n+1}) are needed to determine P'_n by (2-8), the number of data of P'_n is less than P_n by two. If sufficient data are available to apply (2-8) to P'_n again and determine P''_n , P''_n approaches P_∞ more rapidly than P'_n . Then we can get the best value for P_∞ by applying the transformation as many times as we can. In addition it was shown¹⁰ that the transformation can be used to estimate the limit P_∞ , when $\{P_n\}$ satisfies the condition

$$\lim_{n \rightarrow \infty} \frac{P_n - P_\infty}{P_{n-1} - P_\infty} < 1. \quad (2-9)$$

The result is shown in Table 2-2, where we use the data of $\Delta(N)$ for $N = 4, 6, 8, 10, 12, 14$, and 16, and apply the transformation three times. The result of the third transformation in Table 2-2 gives the best estimation we can get, and we determine the error by the difference from the farthest result among the three of the second application of Shanks' transformation. Then we get $\Delta = \epsilon'(0) \equiv \lim_{m \rightarrow 0^+} \epsilon'(m) = 0.411 \pm 0.001$ (Ref. 11). We use this value for Δ in this thesis. Plotting the extrapolated values of $\epsilon'(m)$, we get the magnetization curve at the thermodynamic limit based on (2-4) in Fig. 2-4. As mentioned above the errors are so small that we do not show them explicitly here. The solid lines near H_{c1} and H_{c2} show the anomalous (nonlinear) behaviors of magnetization which will be given later.

§2. 3. 2 Field Derivative

The field derivative $\frac{dm}{dH}$ is derived from

$$\frac{dm}{dH} = \frac{1}{\epsilon''(m)}, \quad (2-10)$$

in the thermodynamic limit. In order to estimate $\epsilon''(m)$, we use the asymptotic form

$$\begin{aligned} & N[(E(N, M+1) - E(N, M)) - (E(N, M) - E(N, M-1))] \\ & \sim \epsilon''(m) + \left[\frac{1}{12}\epsilon^{(4)}(m) + A''(m)\right] \frac{1}{N^2} + O\left(\frac{1}{N^4}\right). \end{aligned} \quad (2-11)$$

Extrapolating the quantity of the left-hand side of (2-11) by the same method as $\epsilon(m)$ (fitting $\epsilon''(m) + \text{constant}/N^2$), we can estimate $\epsilon''(m)$. We have checked that errors are less than a few percent by the same analysis as $\epsilon(m)$. The field derivative curve is shown in Fig. 2-5.

§2. 4 Anomalies at H_{c1} and H_{c2}

Now we want to know the value of $\epsilon''(0) \equiv \lim_{m \rightarrow 0+} \epsilon''(m)$ and $\epsilon''(1) \equiv \lim_{m \rightarrow 1-} \epsilon''(m)$. In order to estimate $\epsilon''(1)$, we use the form

$$\begin{aligned} E(N, N-1) - E(N, N-2) \\ \sim \epsilon'(1) - \frac{3}{2}\epsilon''(1)\frac{1}{N} + \left[\frac{7}{6}\epsilon'''(1) + A'(1)\right]\frac{1}{N^2} + O\left(\frac{1}{N^3}\right). \end{aligned} \quad (2-12)$$

Since $\epsilon'(1) \equiv \lim_{m \rightarrow 1-} \epsilon'(m) = 4$, we can estimate $\epsilon''(1)$ by extrapolating $N[4 - (E(N, N-1) - E(N, N-2))]$ linearly with respect to $1/N$, as shown in Fig. 2-6. The result is $\epsilon''(1) = 0.01 \pm 0.01$. Thus we conclude $\epsilon''(1) = 0$, that is $\frac{dm}{dH} \rightarrow \infty$ at H_{c2} . The form of the anomaly at H_{c2} has been predicted as

$$m \sim 1 - \frac{2}{\pi} \left(1 - \frac{H}{H_{c2}}\right)^{1/2}, \quad (2-13)$$

by a Bethe-ansatz approach¹². Assuming that the form is $m \sim 1 - C(1 - H/H_{c2})^\beta$, and using the values of $\epsilon''(5/6)$ and $\epsilon''(7/8)$ estimated by our analysis, we get $C = 0.66$ and $\beta = 0.51$. Thus our result is almost consistent with (2-13).

At last we determine $\epsilon''(0)$. Now we assume that $\epsilon(m)$ is continuous at $m = 0$, and finite-size correction of $E(N, 0)/N$ is less than $1/N^2$, that is

$$\frac{1}{N}E(N, 0) \sim \epsilon(0) + o\left(\frac{1}{N^2}\right), \quad (2-14)$$

where $\epsilon(0) \equiv \lim_{m \rightarrow 0+} \epsilon(m)$. The absence of a correction larger than $1/N^2$ is supported by the plot of $E(N, 0)/N$ versus $1/N^2$ in Fig. 2-1.

Actually it has been reported that the correction decays faster than $1/N^3$ by an analysis up to $N = 14$ (Ref. 7).

The conformal field theory⁵ gives the relation

$$A(m) \propto v_S(m), \quad (2-15)$$

where $v_S(m)$ is the sound velocity, which is the derivative of the dispersion curve at the origin. Since a recent Monte Carlo calculation¹³ suggested that the dispersion curve near $k = \pi$ has $E \sim ((k - \pi)^2 + \xi^{-2})^{1/2}$ for $\sum_j S_j^z = 1$, it is expected to lead to $\lim_{m \rightarrow 0^+} v(m) = 0$. Thus we assume

$$A(0) \equiv \lim_{m \rightarrow 0^+} A(m) = 0. \quad (2-16)$$

Using (2-3), (2-14) and (2-16), we get

$$E(N, 1) - E(N, 0) \sim \epsilon'(0) + \epsilon''(0) \frac{1}{N} + o\left(\frac{1}{N}\right), \quad (2-17)$$

where $\epsilon'(0) \equiv \lim_{m \rightarrow 0^+} \epsilon'(m)$ and $\epsilon''(0) \equiv \lim_{m \rightarrow 0^+} \epsilon''(m)$. On the other hand the plot of $E(N, 1) - E(N, 0)$ versus $1/N$ in Fig. 2-3 suggests that the finite-size correction decays faster than $1/N$. Therefore we conclude $\epsilon''(0) = 0$ and $\frac{d\epsilon}{dH} \rightarrow \infty$ at H_{c1} . If higher-order derivatives of $\epsilon(m)$ at $m = 0$ can be estimated, the form of divergence at H_{c1} can be determined. But it is difficult to estimate $\epsilon'''(0)$ from $E(N, M)$ up to $N = 16$, which is too small.

As discussed above, we can find the existence of an anomaly at H_{c1} but cannot determine its asymptotic form from the direct analy-

sis of $\epsilon(m)$ based on finite-size data up to $N = 16$. We will determine the anomalous form by another method in the next chapter.

¹ J. N. Imry and J. P. Doyne, *Phys. Rev. Lett.* **48**, 1722 (1982).

² T. G. Th. Halverson, *Phys. Rev. Lett.* **55A**, 207 (1985); *Phys. Rev. Lett.* **58**(11), 1187 (1987).

³ J. L. Cardy, in *Phase Transitions and Critical Phenomena*, edited by C. Domb and D. L. Leiberman (Academic, London, 1982), Vol. 10, Chap. 2, p. 31.

⁴ J. L. Cardy, *J. Phys. A* **12**, 1099 (1979); E. W. Fisher, J. L. Cardy, and M. R. Nightingale, *Phys. Rev. Lett.* **48**, 112 (1982); *J. Appl. Prob.* **24**, 746 (1987).

⁵ J. H. Van den Bergh and L. W. Schwartz, *SIAM J. Math. Anal.* **10**, 389 (1979).

⁶ D. Frascella, *Phys. Rev. Lett.* **52**, 2127 (1984).

⁷ D. Ghatak, *J. Math. Phys.* **24**, 1 (1983).

⁸ M. W. Maier, in *Phase Transitions and Critical Phenomena*, edited by C. Domb and D. L. Leiberman (Academic, London, 1982), Vol. 8, Chap. 8, p. 145.

⁹ D. A. Stahl and W. F. Ford, *SIAM J. Numer. Anal.* **18**, 221 (1981).

¹⁰ T. Nishii and M. Takahashi, *Phys. Rev. Lett.* **66**, 1099 (1981).

¹¹ R. F. Wegner and J. B. Delfino, *J. Phys. C* **14**, 6345 (1981).

References

- ¹ T. Sakai and M. Takahashi, Phys. Rev. **B43**, 13383 (1991).
- ² J. B. Parkinson and J. C. Bonner, Phys. Rev. **B32**, 4703 (1985).
- ³ F. D. M. Haldane, Phys. Lett. **93A**, 464 (1983); Phys. Rev. Lett. **50**, 1153 (1983).
- ⁴ J. L. Cardy, in *Phase Transitions and Critical Phenomena*, edited by C. Domb and D. L. Lebowitz (Academic, London, 1987), Vol. 11, Chap. 2, p. 55.
- ⁵ J. L. Cardy, J. Phys. **A17**, L385 (1984) ; H. W. Blöte, J. L. Cardy, and M. P. Nightingale, Phys. Rev. Lett. **56**, 742 (1986) ; I. Affleck, *ibid.* **56**, 746 (1986).
- ⁶ J. M. Vanden Broeck and L. W. Schwartz, SIAM J. Math. Anal. **10**, 658 (1979).
- ⁷ H. Betsuyaku, Phys. Rev. **B34**, 8125 (1986).
- ⁸ D. Shanks, J. Math. Phys. **34**, 1 (1955).
- ⁹ M. N. Barber, in *Phase Transitions and Critical Phenomena*, edited by C. Domb and D. L. Lebowitz (Academic, London, 1987), Vol. 8, Chap. 2, p. 145.
- ¹⁰ D. A. Smith and W. F. Ford, SIAM J. Numer. Anal. **16**, 223 (1979).
- ¹¹ T. Sakai and M. Takahashi, Phys. Rev. **B42**, 1090 (1990).
- ¹² R. P. Hodgson and J. B. Parkinson, J. Phys. **C18**, 6385 (1985).

¹³ M. Takahashi, Phys. Rev. **B38**, 5188 (1988).

β	$\langle S^2 \rangle$					
1	0.0000	0.0000	0.0000	0.0000	0.0000	0.0000
2	0.0000	0.0000	0.0000	0.0000	0.0000	0.0000
3	0.0000	0.0000	0.0000	0.0000	0.0000	0.0000
4	0.0000	0.0000	0.0000	0.0000	0.0000	0.0000
5	0.0000	0.0000	0.0000	0.0000	0.0000	0.0000
6	0.0000	0.0000	0.0000	0.0000	0.0000	0.0000
7	0.0000	0.0000	0.0000	0.0000	0.0000	0.0000
8	0.0000	0.0000	0.0000	0.0000	0.0000	0.0000
9	0.0000	0.0000	0.0000	0.0000	0.0000	0.0000
10	0.0000	0.0000	0.0000	0.0000	0.0000	0.0000
11	0.0000	0.0000	0.0000	0.0000	0.0000	0.0000
12	0.0000	0.0000	0.0000	0.0000	0.0000	0.0000
13	0.0000	0.0000	0.0000	0.0000	0.0000	0.0000
14	0.0000	0.0000	0.0000	0.0000	0.0000	0.0000
15	0.0000	0.0000	0.0000	0.0000	0.0000	0.0000

Table 2-1 : Numerical results of the lowest energy $E(N, M)$ of $\sum_j S_j \cdot S_{j+1}$ in the subspace where $M = \sum_j S_j^z$ for N -site systems.

N	6	8	10	12	14	16
0	-8.6174	-11.3370	-14.0941	-16.8696	-19.6551	-22.4468
1	-7.8968	-10.7434	-13.5693	-16.3854	-19.1962	-22.0040
2	-6.4617	-9.5966	-12.2597	-15.5294	-18.4227	-21.2916
3	-4.2988	-7.8756	-11.1548	-14.2781	-17.3097	-20.2830
4	-1.4893	-5.6381	-9.2775	-12.6524	-15.8693	-18.9844
5	2	-2.9174	-6.9946	-10.6729	-14.1157	-17.4056
6	6	0.2984	-4.3257	-8.3592	-12.0641	-15.5578
7		4	-1.2672	-5.7244	-11.7284	-13.4527
8		8	2.1938	-2.7674	-9.1177	-11.1005
9			6	0.5232	-6.2319	-8.5076
10			10	4.1355	-3.0632	-5.6747
11				8	2.3902	-2.5965
12				12	6.0999	0.7321
13					10	4.3014
14					14	8.0767
15						12
16						16

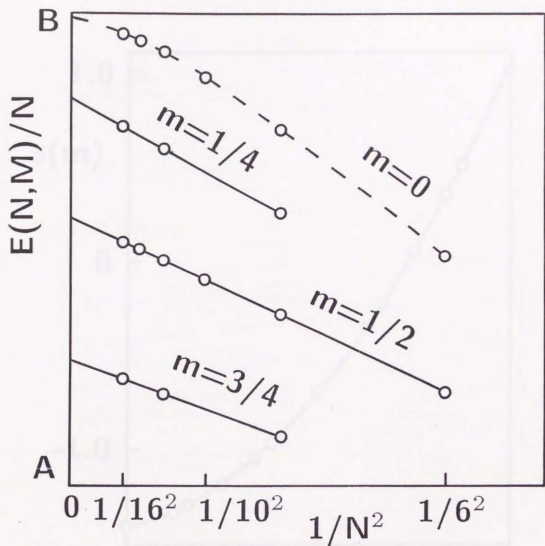


Fig. 2-1. Plots of $E(N, M)/N$ versus $1/N^2$ with $m = M/N = 0, 1/4, 1/2,$ and $3/4$ fixed respectively. The origin is sifted along the vertical axis without changing the scale. The values of points A and B are as follows; A : $-1.47, -1.24, -0.73, -0.03$; B : $-1.40, -1.17, -0.66, -0.10$ for $m = 0, 1/4, 1/2,$ and $3/4$ respectively. The plots are almost linear for $m \neq 0$, which suggests that the lowest-energy states are massless.

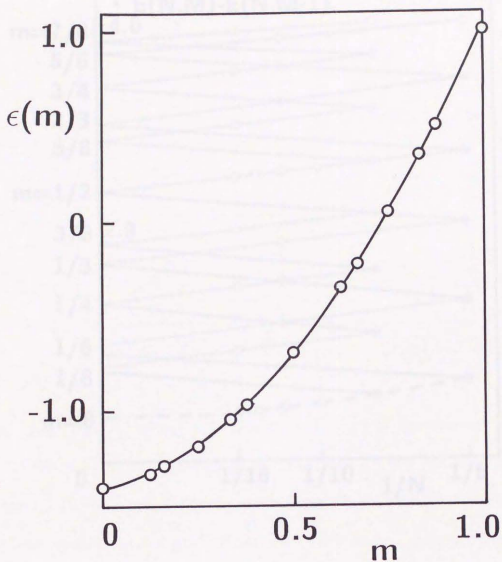


Fig. 2-2. Plot of the lowest energy per site $\epsilon(m)$ versus m . Each point is derived from the largest- and next-largest-size data of $E(N, M)/N$ using the extrapolating form (2-3). The solid curve is only a guideline. As mentioned in the text the error of each point is so small (we think it is within 0.1%) that we do not write it explicitly.

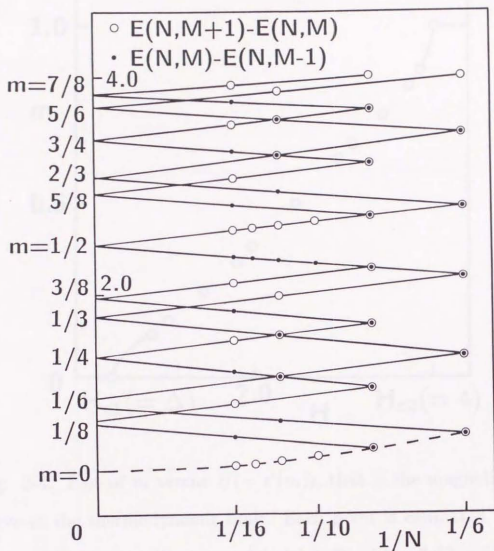


Fig. 2-3. Plots of spin-excitation gap versus $1/N$ with $m = M/N$ fixed. The plots are almost linear for $m = 1/4, 1/2$, and $3/4$. For $m \neq 0$, $E(N, M+1) - E(N, M)$ and $E(N, M) - E(N, M-1)$ coincide well at the thermodynamic limit ($N \rightarrow \infty$). For $m = 0$, the gap $E(N, 1) - E(N, 0)$, which are connected by a dashed curve, converges faster than $1/N$ and has a finite value $\Delta = 0.411 \pm 0.001$ (this is the result of by Shanks' transformation) in the thermodynamic limit.

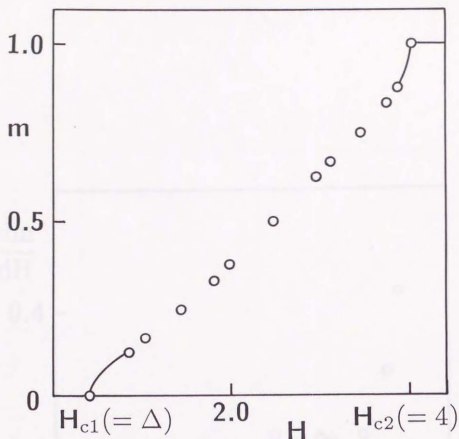


Fig. 2-4. Plot of m versus $H(= \epsilon'(m))$, that is the magnetization curve at the thermodynamic limit. Each point is estimated by averaging the two results extrapolated by (2-5) and (2-6). For the extrapolation, we use the largest- and next-largest-size data of $E(N, M+1) - E(N, M)$ and $E(N, M) - E(N, M-1)$, respectively. We estimate the error of each point by the difference between the two results extrapolated by (2-5) and (2-6), but it is so small (less than a few percent) that we do not write it explicitly. We use $H_{c1} = 0.411$ which is the result of shanks' transformation. Solid lines are drawn based the forms (3-15) and (3-16) from the nearest points, as mentioned in chapter 3.

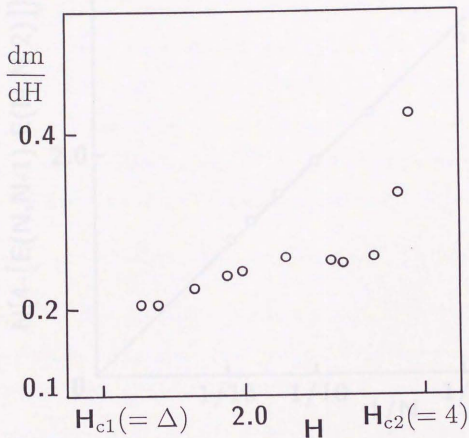


Fig. 2-5. Curve of the field derivative $\frac{dm}{dH}$ ($= 1/\epsilon''(m)$) at the thermodynamic limit derived from the extrapolation (2-11). We apply the same extrapolation as $\epsilon(m)$ to estimate $\epsilon''(m)$ here. The error is so small (less than a few percent) that we do not write it explicitly.

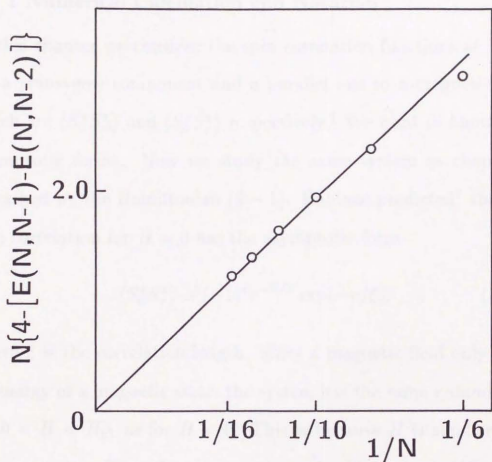


Fig. 2-6. Plot of $N\{4 - (E(N, N - 1) - E(N, N - 2))\}$ versus $1/N$. The extrapolated value is 0.01 ± 0.01 . This result is estimated from the two points for $N = 14$ and $N = 16$ by $1/N$ -linear extrapolation, and the error is the difference from the result for $N=12$ and 14 . It suggests $\epsilon''(1) = 0$.

Chapter 3. Spin Correlation

§3. 1 Numerical Calculation and Notation

In this chapter we consider the spin correlation functions at $T = 0$ for a transverse component and a parallel one to a magnetic field, which are $\langle S_0^x S_r^x \rangle$ and $\langle S_0^z S_r^z \rangle$ respectively.¹ We want to know their asymptotic forms. Now we study the same system as chapter 2, described by the Hamiltonian (2-1). Haldane predicted² that the spin correlation for $H = 0$ has the asymptotic form

$$\langle S_0^z S_r^z \rangle \simeq (-1)^r r^{-1/2} \exp(-r/\xi), \quad (3-1)$$

where ξ is the correlation length. Since a magnetic field only shifts an energy of a magnetic state, the system has the same ground state for $0 < H < H_{c1}$ as for $H = 0$. This is because H is smaller than the energy gap. Thus the spin correlation is still isotropic ($\langle S_0^x S_r^x \rangle = \langle S_0^z S_r^z \rangle$) and has the same asymptotic form (3-1) for $0 < H < H_{c1}$. But the magnetized ground state for $H_{c1} < H < H_{c2}$ is massless, as shown in chapter 2, and then it is expected that the spin correlation decays algebraically. We estimate the correlation exponent in this chapter.

In order to estimate the correlation exponent, we use the relation between the size dependence of the excitation energy gap and the exponent, which is predicted from the conformal field theory.³

Using the Lanczos algorithm, we calculate the lowest-state energy of \mathcal{H}_0 in the subspace where the system has the magnetization $\sum_j S_j^z = M$ and wave vector k , for the N -lattice system under the periodic boundary condition. We restrict N to an even integer and $N \leq 16$ again. We define the energy as $E_k(N, M)$. In addition we define the lowest one among $E_k(N, M)$'s corresponding to all values of k , as $E(N, M)$. The definition of $E(N, M)$ is same as chapter 2. In this case, $E(N, M) = E_0(N, M)$ for even M and $E(N, M) = E_\pi(N, M)$ for odd M (ref. 4).

§3. 2 Prediction from Conformal Invariance

In this section we give a brief review of the result from the conformal invariance which we use in this chapter.

We consider the one-dimensional quantum system with the field $\phi(r)$ under the periodic boundary condition, which has size N , and a ground state $|0\rangle$ with the energy E_N^0 , where $|0\rangle$ is massless in the thermodynamic limit. We define E_N^ϕ is the lowest energy of the excited state $|\phi\rangle$ with the non-zero matrix element $\langle 0|\phi(0)|\phi\rangle \neq 0$. The conformal field theory predicts⁵ that the asymptotic behavior of the ground state energy and excitation energy gap for $N \rightarrow \infty$ have the forms

$$E_N^0 \simeq N\epsilon_0 - \frac{\pi}{6}cv_S \frac{1}{N} + O\left(\frac{1}{N^2}\right) \quad (3-2)$$

$$E_N^\phi - E_N^0 \simeq 2\pi v_S \theta \frac{1}{N}, \quad (3-3)$$

where c is the central charge in the Virasoro algebra⁶ satisfied by the energy-momentum tensor, v_S is the sound velocity which is the derivative of the dispersion curve at the origin, and θ is the conformal dimension of $\phi(r)$. The form of the finite-size correction (2-3) is derived from (3-2). The conformal dimension θ determines the asymptotic form of the correlation function in the ground state as follows:

$$\langle 0|\phi(0)\phi(r)|0\rangle \simeq r^{-2\theta}. \quad (3-4)$$

Thus the correlation exponent can be estimated from the size dependence of the energy gap.

For the critical behavior of Δ we do not need the exact solution of $\mathcal{F}(T, T_c)$ for two-dimensional random systems at $T = T_c$. There is only one set of values of ν which is allowed by universality of the scaling exponent. This is $\nu = 2/(d+2)$ (Eqs. 2-3) as follows. The only ν for which the exponent ν has continuously diverged as the parameter of the model² (for example, the two-dimensional Ising model has $\nu = 1/2$ and the two-dimensional Ising model and the $d = 1, 2$ spin-dimensional Ising model have $\nu = 1$).

In order to determine the critical change of the model (2-1) for $d < 4$ in $\nu = 1$, we use the asymptotic behavior of the ground state energy derived from (2-3), which is

$$\frac{1}{2} \int_0^{\infty} \mathcal{F}(X, 0) dx \sim \frac{1}{2} \int_0^{\infty} \frac{dx}{x^{\nu}} \quad (2-4)$$

where we omit the term $-E_0$ which does not depend on β . The term corresponds to (2-3), which has been checked to be identical to $\mathcal{F}(X, 0)$ as shown in Fig. 2-1 in chapter 2. In order to determine the value of ν , we estimate the gradient of the plot $E(N_s, 0)/N_s$ versus $(N_s)^{-1/2}$ in Fig. 2-1, which denotes $A = \nu \ln(2)/\beta$, and the ground velocity $v_g = \Delta_0 v_g$ is the gradient of the dispersion curve at $k=0$ (right), so we have $v_g = \Delta_0$.

$$v_g = \frac{1}{2} (E_N(X, 0) - E(N, 0)) \quad (2-5)$$

§3. 3 Central Charge

The central charge c parametrizes the conformal field theory describing the critical behavior of a two-dimensional classical system at $T = T_c$, or a one-dimensional massless quantum system at $T = 0$. For $c < 1$ a discrete set of values of c is allowed by unitarity of the scaling operator,⁷ that is $c = 1 - 6/[m(m+1)]$ ($m \geq 2$ an integer). For $c = 1$ the critical exponents may continuously depend on the parameters of the model.⁸ For example, the two-dimensional Ising model has $c = 1/2$, and the two-dimensional classical XY model and the $S = 1/2$ one-dimensional Heisenberg model have $c = 1$.

In order to determine the central charge of the model (2-1) for $0 < m < 1$, we use the asymptotic behavior of the ground state energy derived from (3-2), which is

$$\frac{1}{N}E(N, M) \simeq \epsilon(m) - \frac{\pi}{6}cv_S \frac{1}{N^2} \quad (N \rightarrow \infty), \quad (3-5)$$

where we omit the term $-Hm$ which exists on both hand sides. The form corresponds to (2-3), which has been checked to be satisfied for $0 < m < 1$ as shown in Fig. 2-1 in chapter 2. In order to determine the value of c , we estimate the gradient of the plot $E(N, M)/N$ versus $1/N^2$ in Fig. 2-1, which denotes $A = \pi cv_S/6$, and the sound velocity v_S . As v_S is the gradient of the dispersion curve at the origin, we estimate v_S by

$$v_S = \frac{N}{2\pi}(E_{k_1}(N, M) - E(N, M)), \quad (3-6)$$

where $k_1 = 2\pi/N$ for even M and $k_1 = \pi - 2\pi/N$ for odd M . We have found that the size correction of (3-6) is not $O(1/N)$ but $O(1/N^2)$ numerically for $m=1/4, 1/2,$ and $3/4$, which means that the dispersion has the form $C_1k + C_2k^3$ ($k \rightarrow 0$) (C_1 and C_2 are constants). It is similar to the dispersion for $S = 1/2$ which has the form $|\sin k|$ (Ref. 9). We use the value of v_S for $N = 16$ ($N = 12$ only for $m=1/6, 1/3, 2/3,$ and $5/6$) and neglect the size correction here (at least we checked that the error due to the size correction is less than 1% for $m=1/4, 1/2,$ and $3/4$). In order to estimate A , we use the two values of $E(N, M)$ for the largest N and next largest N such that magnetization is $m = M/N$ up to $N = 16$, and neglect the size correction. For example, we use $E(16, 4)$ and $E(12, 3)$ for $m = 1/4$, and use $E(12, 2)$ and $E(6, 1)$ for $m=1/6$. Using those values of v_S and A , we estimate the central charge c for $m=1/8, 1/6, 1/4, 1/3, 3/8, 1/2, 5/8, 2/3, 3/4, 5/6,$ and $7/8$, and plot them in Fig. 3-1. It suggests that $c = 1$ for $0 < m < 1$. Thus the critical exponents can vary with the magnetization m .

§3. 4 Spin Correlation Exponents

§3. 4. 1 Transverse Spin Correlation

Now we consider the spin correlation exponent in the magnetic state ($0 < m < 1$) at $T = 0$. First we investigate the correlation function of the transverse component to a magnetic field, which is $\langle S_0^x S_r^x \rangle$. As the system is massless for $0 < m < 1$, the asymptotic form of the transverse spin correlation decays algebraically and is assumed to be

$$\langle S_0^x S_r^x \rangle \simeq (-1)^r r^{-\eta} \quad (r \rightarrow \infty), \quad (3-7)$$

in the thermodynamic limit. Then we determine the correlation exponent η . When we apply the conformal field theory to the Hamiltonian \mathcal{H} of (2-1), E_N^0 and E_N^ϕ correspond to $E(N, M) - HM$ and $E(N, M + 1) - H(M + 1)$ respectively. Then the relation (3-3) leads to the size dependence of spin-excitation energy gap

$$E(N, M + 1) - E(N, M) - H \simeq \pi v_S \eta \frac{1}{N} \quad (N \rightarrow \infty). \quad (3-8)$$

We have checked numerically that the gap is linear with respect to $1/N$ in Fig. 2-3. Here, in order to estimate η , we eliminate H , subtracting the energy of the spin excitation ($M - 1 \rightarrow M$) from eq. (3-8) and get

$$\begin{aligned} & [E(N, M + 1) - E(N, M)] - [E(N, M) - E(N, M - 1)] \\ & \simeq 2\pi v_S \eta \frac{1}{N} \quad (N \rightarrow \infty). \end{aligned} \quad (3-9)$$

Using the form of v_s (3-6), we get the relation

$$\eta = \frac{E(N, M+1) + E(N, M-1) - 2E(N, M)}{E_{k_1}(N, M) - E(N, M)}. \quad (3-10)$$

We use eq. (3-10) to estimate η . Estimated η for $N = 16$ and $N = 12$ is plotted versus magnetization m in Fig. 3-2, which shows that each value of η converges well with respect to the system size N . We have found that the size correction of eq. (3-10) behaves as $O(1/N^2)$ numerically, but we neglect the correction because it is small (at least, we checked that the correction for $N = 16$, which was estimated from the difference between the values of η for $N = 16$ and $N = 14$, is less than a few percents for $m = 1/4, 1/2$, and $3/4$). In addition we determine η in the limits of $m \rightarrow 0+$ and $m \rightarrow 1-$, extrapolating the value of η for $M = 1$ and $M = N - 1$ linearly to $1/N$, as shown in Fig. 3-3. We take the value extrapolated from $N = 14$ and 16 for the best estimation, and take the difference from the value extrapolated from $N = 12$ and 14 for the error of extrapolation. The results are $\eta = 0.493 \pm 0.009$ for $m = 0$ and $\eta = 0.499 \pm 0.003$ for $m = 1$. Thus, we conclude that $\eta = 1/2$ for $m = 0$ and 1 . It is consistent with Schulz's statement.¹⁰ He conjectured that $\eta = 1/2$ at H_{c1} , by representing a spin-1 operator as the sum of two spin-1/2 operators.

§3. 4. 2 Parallel Spin Correlation

Next we consider the correlation function of the parallel component to a magnetic field. In the magnetic state ($0 < m < 1$), finite magnetization exists along the z -axis and a gapless excitation (gap decays as $\Delta \simeq 1/N$) can exist at the soft mode of $k = 2k_F$. In this case, $2k_F = 2\pi M/N$ for even M and $2k_F = \pi - 2\pi M/N$ for odd M . The existence of the soft mode is based on the assumption that the magnetic state can be described by an interacting fermion model where the number of the fermion is given by M . The assumption will be supported by the consistency with the Luttinger liquid concept in the next section. In this case, the asymptotic behavior of the correlation function for the parallel component is expected to be

$$\langle S_0^z S_r^z \rangle - m^2 \simeq \cos(2k_F r) r^{-\eta^z} \quad (r \rightarrow \infty). \quad (3-11)$$

The conformal field theory can also be applied to this case¹¹ and the energy gap of the soft mode depends on the system size as

$$E_{2k_F}(N, M) - E(N, M) \simeq \pi v_S \eta^z \frac{1}{N} \quad (N \rightarrow \infty). \quad (3-12)$$

According to our numerical check for $m = 1/4, 1/2$, and $3/4$ up to $N = 16$, the asymptotic form $E_{2k_F}(N, M) - E(N, M) \simeq 1/N$ is satisfied within the error, as shown in Fig. 3-4 (Unfortunately the error is very large for $m = 1/4$). Thus we assume that the gapless

excitation exists at $2k_F$. Now we determine the exponent η^z . Using eqs. (3-6) and (3-12), we get

$$\eta^z = 2 \frac{E_{2k_F}(N, M) - E(N, M)}{E_{k_1}(N, M) - E(N, M)}. \quad (3-13)$$

The results of η^z estimated by (3-13) for $N = 12$ and 16 are plotted in Fig. 3-5. These converge well with respect to the system size. We checked that the size correction of (3-13) decays as $o(1/N)$ numerically, but neglect it here. The values of η^z for $M = 1$ and $M = N - 1$ are 2 by definition (3-13), and they are independent of N . Thus we conclude that $\eta^z = 2$ for $m = 0$ and $m = 1$ in the thermodynamic limit.

As shown in Figs. 3-2 and 3-5, the exponent η has a minimum and η^z has a maximum at $m \simeq 1/3$. Thus, the transverse spin correlation is strong and the parallel one is weak there. In addition, we conclude that $\eta = 1/2$ and $\eta^z = 2$ for $m = 0$ and $m = 1$, as discussed above. It is noted that such behavior of the exponents η and η^z is very different from the case of $S = 1/2$. According to the exact approach for $S = 1/2$, the system has a massless ground state at $H = 0$, and both correlation exponents η and η^z are one at $m = 0$ (Ref. 12). The ground state is still massless for $H > 0$. As H increases, η decreases monotonously to $1/2$ ($H = H_{c2} = 2$), and η^z increases monotonously to 2 ($H = H_{c2}$) for $S = 1/2$ (Ref. 13).

§3. 5 Luttinger Liquid Concept

Finally, we consider the Luttinger liquid concept.¹⁴ Haldane suggested that the Luttinger liquid can describe many one-dimensional quantum systems with gapless excitations, and the validity has already been checked for some exactly solvable models, for example, the $S = 1/2$ XXZ spin chain¹⁴ and the Hubbard chain.¹⁵⁻¹⁷

Now we consider an interacting spinless Fermion system as an example of the Luttinger liquid. The Luttinger liquid theory assumes that the elementary excitation can be described by the Hamiltonian

$$\mathcal{H}_L = v_S \sum_k |k| b_k^\dagger b_k + \frac{1}{2} \frac{\pi}{L} [v_N (N - N_0)^2 + v_J J^2], \quad (3-14)$$

where v_S is the sound velocity (the derivative of the dispersion), b_k is the Boson operator, L is the system size, N_0 is the number of the Fermions, $N - N_0$ is the number of the extra Fermions, and J is the number of the particle-hole pair excitations with the wave vector $2k_F$ ($k_F = \pi N_0/L$). The last two terms of (3-14) are the energy gaps of the charge excitation and the $2k_F$ current excitation respectively, and these excitations are gapless in the thermodynamic limit. The parameters v_N and v_J are the velocities associated with the charge and current excitations respectively, and they are given by the forms $v_N = v_S e^{-2\varphi}$ and $v_J = v_S e^{2\varphi}$ where φ is the parameter determined from the interaction of the original system. Thus the relation

$$v_S = (v_N v_J)^{1/2}, \quad (3-15)$$

is satisfied. For the non-interacting spinless Fermion system ($\varphi = 0$) the three velocities v_S , v_N , and v_J all correspond to the Fermi velocity v_F . The important statement of the Luttinger liquid theory is that the effect of the interaction is only to change the values of v_S and φ , as far as the low-energy excitation is considered.

Our numerical check for the system (2-1) suggests the existence of the two gapless excitations, which are the spin excitation and $2k_F$ excitation respectively. It implies that the magnetization of the $S = 1$ antiferromagnetic Heisenberg chain corresponds to the charge of the Luttinger liquid. If the magnetic state of an $S = 1$ antiferromagnetic Heisenberg chain is described by the Luttinger liquid through the correspondence, the velocities v_N and v_J are expected to be given by the relation

$$v_N = \lim_{N \rightarrow \infty} \frac{N}{\pi} [(E(N, M+1) - E(N, M)) - (E(N, M) - E(N, M-1))], \quad (3-16)$$

$$v_J = \lim_{N \rightarrow \infty} \frac{N}{2\pi} [E_{2k_F}(N, M) - E(N, M)]. \quad (3-17)$$

The Luttinger liquid theory can give the correlation exponents as

$$\eta = \frac{1}{2} v_N / v_S, \quad (3-18)$$

$$\eta^z = 2v_J / v_S. \quad (3-19)$$

These forms correspond to (3-10) and (3-13) given by the conformal invariance in the thermodynamic limit. If the Luttinger liquid theory

is valid, the relation

$$\eta\eta^z = 1, \quad (3-20)$$

which is derived from (3-15), (3-18), and (3-19), should be satisfied. To check this, we show the value of $\eta\eta^z$ calculated by (3-10) and (3-13) for each M in the case of $N = 16$ in Table 3-1. It shows that relation (3-20) is well satisfied. Thus the behaviors of the magnetic state of an $S = 1$ antiferromagnetic Heisenberg chain are consistent with the Luttinger liquid.

§3. 6 Anomalies of Magnetization Curve

Now assuming the Luttinger liquid concept, we consider the form of the magnetization curve near the limits of $m \rightarrow 0+$ and $m \rightarrow 1-$. It has already been found that two anomalies exist at $m = 0$ and 1. As discussed above, the correlation exponents η and η^z are determined as $\eta = 1/2$ and $\eta^z = 2$ in both limits. According to the Luttinger liquid concept in the last section, $\eta = 1/2$ and $\eta^z = 2$ ($v_S = v_N = v_J = v_F$) mean that the elementary excitation is described by a free-Fermion system, which has a dispersion which behaves like k^2 .

If we assume such a dispersion, the forms of the magnetization curve near the two limits are derived as (Ref. 18)

$$m \simeq (H - H_{c1})^{1/2} \quad (m \rightarrow 0+), \quad (3-21)$$

$$1 - m \simeq (H_{c2} - H)^{1/2} \quad (m \rightarrow 1-), \quad (3-22)$$

where $H_{c1}(= \Delta)$ is the transition point from the nonmagnetic to magnetic state, and $H_{c2}(= 4)$ is the point where magnetization is saturated, as discussed in chapter 2. Relations (3-21) and (3-22) are consistent with some phenomenological approaches.¹⁹⁻²¹ In addition (3-22) is consistent with the result of the Bethe-ansatz approach (2-13)(Ref. 22).

References

- ¹ T. Sakai and M. Takahashi, J. Phys. Soc. Jpn. **60**, 3615 (1991).
- ² F. D. M. Haldane, Phys. Lett. **93A**, 464 (1983); Phys. Rev. Lett. **50**, 1153 (1983).
- ³ J. L. Cardy, in *Phase Transitions and Critical Phenomena*, edited by C. Domb and D. L. Lebowitz (Academic, London, 1987), Vol. 11, Chap. 2, p. 55.
- ⁴ J. B. Parkinson and J. C. Bonner, Phys. Rev. **B32**, 4703 (1985).
- ⁵ J. L. Cardy, J. Phys. **A17**, L385 (1984) ; H. W. Blöte, J. L. Cardy, and M. P. Nightingale, Phys. Rev. Lett. **56**, 742 (1986) ; I. Affleck, *ibid.* **56**, 746 (1986).
- ⁶ A. A. Belavin, A. M. Polyakov, and A. B. Zamolodchikov, Nucl. Phys. **B241**, 333 (1984).
- ⁷ D. Friedan, Z. Qiu, and S. H. Shenker, Phys. Rev. Lett. **52**, 1575 (1984).
- ⁸ A. B. Zamolodchikov and V. A. Fateev, JETP, **62**, 215 (1985).
- ⁹ J. des Cloizeaux and J. J. Pearson, Phys. Rev. **128**, 2131 (1962).
- ¹⁰ H. J. Schulz, Phys. Rev. **B34**, 6372 (1986).
- ¹¹ N. M. Bogoliubov, A. G. Izergin and N. Yu Reshetikhin, J. Phys. **A20**, 5361 (1987).
- ¹² A. Luther and I. Peschel, Phys. Rev. **B12**, 3908 (1975).

- ¹³ N. M. Bogoliubov, A. G. Izergin, and V. E. Korepin, Nucl. Phys. **B275** [FS17], 687 (1986).
- ¹⁴ F. D. M. Haldane, Phys. Rev. Lett. **45**, 1358 (1980); Phys. Lett. **81A**, 153 (1981); J. Phys. **C14**, 2585 (1981).
- ¹⁵ N. Kawakami and S. -K. Yang, Phys. Lett. **148A**, 359 (1990).
- ¹⁶ H. Fram and V. E. Korepin, Phys. Rev. **B42**, 10553 (1990).
- ¹⁷ H. J. Schulz, Phys. Rev. Lett. **64**, 2831 (1990).
- ¹⁸ K. Nomura and T. Sakai, Phys. Rev. **B44**, 5092 (1991).
- ¹⁹ A. M. Tselik, Phys. Rev. **B42**, 10499 (1990).
- ²⁰ I. Affleck, Phys. Rev. **B43**, 3215 (1991).
- ²¹ M. Takahashi and T. Sakai, J. Phys. Soc. Jpn. **60**, 760 (1991).
- ²² R. P. Hodgson and J. B. Parkinson, J. Phys. **C18**, 6385 (1985).

Table 3-1 : Exponents η and η^z estimated from (3-10) and (3-13) for $N = 16$, and the value of $\eta\eta^z$. The relation $\eta\eta^z = 1$ is satisfied well.

M	η	η^z	$\eta\eta^z$
1	0.432	2	0.864
2	0.391	2.523	0.986
3	0.368	2.755	1.015
4	0.358	2.873	1.029
5	0.353	2.941	1.037
6	0.351	2.975	1.043
7	0.353	2.974	1.048
8	0.360	2.910	1.048
9	0.375	2.788	1.046
10	0.400	2.589	1.035
11	0.432	2.366	1.022
12	0.464	2.184	1.013
13	0.487	2.072	1.009
14	0.499	2.019	1.008
15	0.504	2	1.007

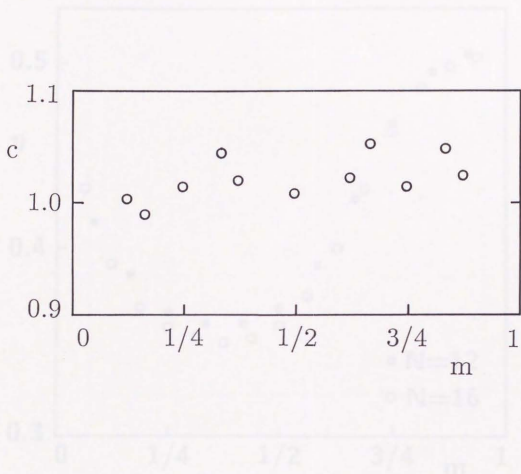


Fig. 3-1. Central charge c estimated from eqs. (3-5) and (3-6). We use the largest-two-size data of $E(N, M)/N$ for $A = \pi cv_S/6$, and the value of v_S for $N = 16$, to estimate c for $m = 1/8, 1/6, 1/4, 1/3, 3/8, 1/2, 5/8, 2/3, 3/4, 5/6$, and $7/8$.

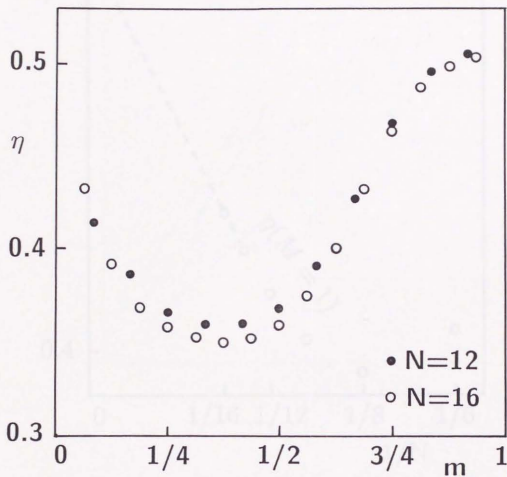


Fig. 3-2. Exponent η estimated from eq. (3-10) for $N=12$ and 16 .

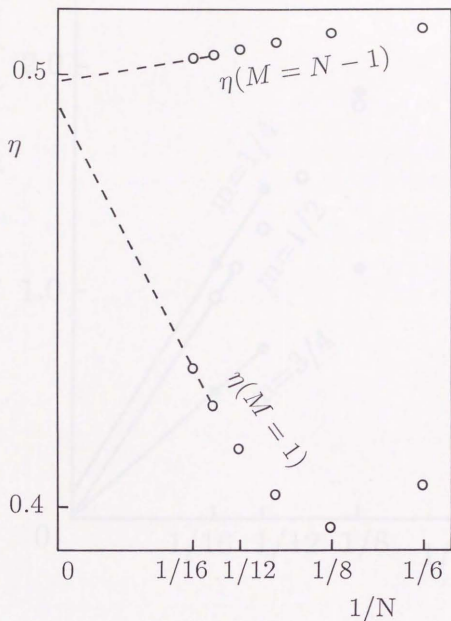


Fig. 3-3. Exponent η for $M = 1$ and $N - 1$ estimated from (3-10), plotted versus $1/N$. Extrapolated results are $\eta = 0.493 \pm 0.009$ for $m = 0$ and $\eta = 0.493 \pm 0.003$ for $m = 1$. Thus we determine $\eta = 1/2$ for both points.

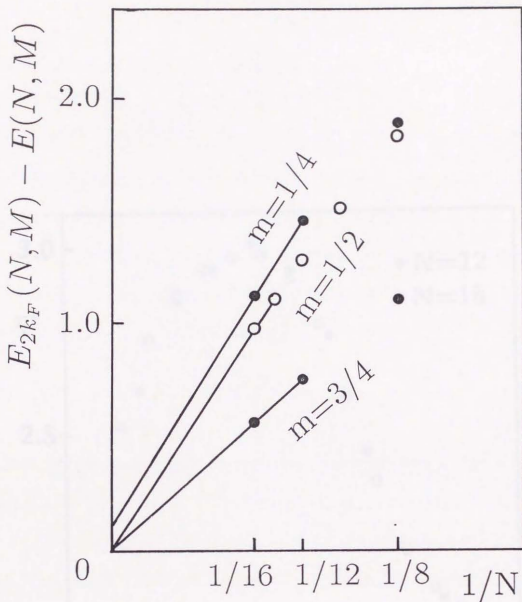


Fig. 3-4. $2k_F$ excitation gap $E_{2k_F}(N, M) - E(N, M)$ plotted versus $1/N$ for $m=1/4, 1/2$, and $3/4$. The estimated values in the thermodynamic limit are 0.1 ± 0.5 , 0.0 ± 0.1 , and 0.0 ± 0.1 for $m=1/4, 1/2$, and $3/4$, respectively. Although the error is very large for $m=1/4$, we assume that the $2k_F$ excitation is gapless for $0 < m < 1$.

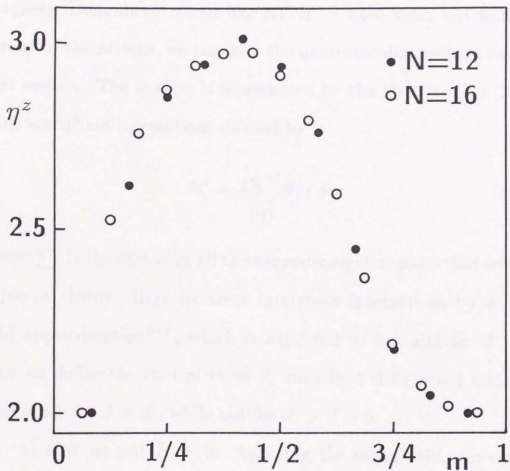


Fig. 3-5 Exponent η^z estimated from eq. (3-13) for $N = 12$ and 16.

Chapter 4. Quasi-One-Dimensional Case

§4. 1 Mean Field Approximation for Interchain Interaction

As most real materials described by the one-dimensional antiferromagnetic Heisenberg model like NENP^{1,2} have weak but finite interchain interactions, we consider the quasi-one-dimensional case³ in this section. The system is represented by the Hamiltonian (2-1) with interchain interactions defined by

$$\mathcal{H}' = J \sum'_{\langle ij \rangle} \mathbf{S}_i \cdot \mathbf{S}_j, \quad (4-1)$$

where \sum' is the sum over all the nearest-neighbor pairs that connect adjacent chains. Here we treat interchain interactions by a mean field approximation⁴⁻⁶, which is expected to be valid for $J \ll 1$. Now we define the critical value J_c such that the ground state has Néel order for $J > J_c$, while not for $J_c > J > 0$.

At first we put $H = 0$. Applying the mean field approximation for interchain interactions, the part of the hamiltonian which is concerned with the i th chain, has the form

$$\mathcal{H}_i = \sum_j \mathbf{S}_{i,j} \cdot \mathbf{S}_{i,j+1} + J \sum_j \mathbf{S}_{i,j} \cdot \sum_{\rho} \langle \mathbf{S}_{\rho,j} \rangle, \quad (4-2)$$

where the subscript i specifies a chain, j is a coordinate along the chain and \sum_{ρ} describes the sum for all the nearest-neighbor chains.

The mean field $\langle \mathbf{S}_{\rho,j} \rangle$ is averaged for ρ th chain, independently of other chains. If the easy axis of staggered magnetization is x -axis, we substitute a mean field

$$\begin{aligned} \langle S_{\rho,j}^x \rangle &= -(-1)^j m_{\text{st}} \\ \langle S_{\rho,j}^y \rangle &= \langle S_{\rho,j}^z \rangle = 0, \end{aligned} \quad (4-3)$$

for $\langle \mathbf{S}_{\rho,j} \rangle$. Then the Hamiltonian (4-1) is replaced by

$$\mathcal{H}_{\text{eff}} = \sum_j \mathbf{S}_j \cdot \mathbf{S}_{j+1} - h_{\text{eff}} \sum_j (-1)^j S_j^x, \quad (4-4)$$

$$h_{\text{eff}} = ZJm_{\text{st}}, \quad (4-5)$$

where Z is the number of adjacent chains ($Z=2$ or 4 for NENP(Ref. 6)) and the subscript i is omitted. This is the effective hamiltonian of the one-dimensional system to which the staggered magnetic field h_{eff} is applied. If for this one-dimensional system the sublattice magnetization in the ground state can be given as the function of h_{eff} such that

$$m_{\text{st}} = f(h_{\text{eff}}), \quad (4-6)$$

then we get the self-consistent equation

$$m_{\text{st}} = f(2Jm_{\text{st}}). \quad (4-7)$$

By solving this equation the sublattice magnetization m_{st} can be obtained. Generally $f(h_{\text{eff}})$ is a concave function and satisfies $f(0) =$

0, and the solution m_{st} is obtained from the intersection of $f(h_{eff})$ and the line h_{eff}/ZJ . Therefore whether a non-zero solution m_{st} exists or not is determined by the gradient of $f(h_{eff})$ at $h_{eff} = 0$, that is the staggered susceptibility

$$\chi_{st}^{xx} = \left(\frac{\partial m_{st}}{\partial h_{eff}} \right)_{h_{eff}=0} . \quad (4-8)$$

If $\chi_{st}^{xx} > 1/ZJ$ then a non-zero solution exists, otherwise not. Therefore the critical value J_c is given by

$$J_c = \frac{1}{Z\chi_{st}^{xx}} . \quad (4-9)$$

Thus within this approximation we have only to calculate the staggered susceptibility for the one-dimensional system at $T = 0$.

When the finite magnetization along z -axis exists, the easy axis of the staggered magnetization is in the xy -plane. Thus the relation (4-9) is valid even for the magnetic state.

§4. 2 Staggered Susceptibility of One-Dimensional System

In order to study the antiferromagnetic property in the plane perpendicular to the magnetic field ($H \parallel S^z$) for the quasi-one-dimensional system, we calculate the staggered susceptibility along x -axis for the one-dimensional system at $T = 0$, which is given by

$$\chi_{st}^{xx} = \lim_{\beta \rightarrow \infty} \beta \langle \hat{M}_{st}^x; \hat{M}_{st}^x \rangle, \quad (\beta \equiv 1/k_B T), \quad (4-10)$$

where

$$\hat{M}_{st}^x \equiv \sum_j (-1)^j S_j^x, \quad (4-11)$$

and $\langle \dots; \dots \rangle$ is the canonical correlation⁷ defined by

$$\langle A; B \rangle \equiv \frac{\int_0^\beta d\lambda \text{Tr}[e^{-\beta\mathcal{H}} e^{\lambda\mathcal{H}} A e^{-\lambda\mathcal{H}} B]}{\beta \text{Tr} e^{-\beta\mathcal{H}}}. \quad (4-12)$$

In the form (4-12) \mathcal{H} is the Hamiltonian (2-1). Integrating over λ in the limit $\beta \rightarrow \infty$, we get the form

$$\chi_{st}^{xx} = \frac{2}{N} \sum_l \frac{|\langle l | \hat{M}_{st}^x | g \rangle|^2}{\varepsilon_l - \varepsilon_g}, \quad (4-13)$$

where $|g\rangle$ is the ground state, $|l\rangle$ is the excited state, and $\varepsilon_g, \varepsilon_l$ are their energies, respectively, for the Hamiltonian (2-1) at finite H . We calculate χ_{st}^{xx} of finite systems under periodic boundary condition at $T = 0$ numerically as follows: At first, using the Lanczos algorithm, we get the wave function of the ground state for the Hamiltonian (2-1) with a staggered magnetic field described by

$$\mathcal{H}'' = -h \hat{M}_{st}^x. \quad (4-14)$$

Next we calculate the transverse staggered magnetization $\langle \hat{M}_{st}^x \rangle$ for this state. At last we differentiate it with respect to h numerically to estimate χ_{st}^{xx} . Thus our numerical calculation is based on (4-8) rather than (4-13). We use this method to calculate χ_{st}^{xx} up to $N = 12$. This method can be used to calculate χ_{st}^{xx} at most up to $N = 14$, because $\sum_j S_j^z$ is not conserved owing to the staggered magnetic field (4-14) and the dimension of the Hilbert space used for calculation becomes larger. However the direct calculation based on (4-13) is available only for smaller systems. The behavior of χ_{st}^{xx} for $N = 12$ is shown as a dashed curve in Fig. 4-1. It is found that χ_{st}^{xx} diverges at each level-crossing point, which is defined by $H_M \equiv E(N, M) - E(N, M - 1)$, ($\lim_{N \rightarrow \infty} H_1 = H_{c1}$, $H_N = H_{c2}$). The form of the divergence at each H_M is

$$\chi_{st}^{xx} \sim \frac{1}{|H - H_M|}. \quad (4-15)$$

In particular for $H > H_{c2}$, χ_{st}^{xx} can be calculated analytically because the ground state is completely ferromagnetic here, and we get

$$\chi_{st}^{xx} = \frac{1}{H - H_{c2}} \quad (H > H_{c2}), \quad (4-16)$$

which is independent of N . Now we define the quantity

$$\tilde{\chi}_{st}^{xx} \equiv \frac{2}{N} \frac{|\langle M | \hat{M}_{st}^x | M - 1 \rangle|^2}{H - H_M} + \frac{2}{N} \frac{|\langle M + 1 | \hat{M}_{st}^x | M \rangle|^2}{H_{M+1} - H}, \quad (4-17)$$

for $H_M < H < H_{M+1}$ ($1 \leq M \leq N - 1$). This satisfies the inequality

$$\chi_{st}^{xx} \geq \tilde{\chi}_{st}^{xx}. \quad (4-18)$$

$\tilde{\chi}_{st}^{xx}$ gives a good approximation of χ_{st}^{xx} . According to our check, χ_{st}^{xx} and $\tilde{\chi}_{st}^{xx}$ coincide within 0.4% and the difference between them decreases as H approaches H_M , at least up to $N = 14$. Since the system (2-1) is massless between H_{c1} and H_{c2} as shown in chapter 2, we think that χ_{st}^{xx} always diverges in this region, as shown by the solid curve in Fig. 4-1. In order to make sure of it, we check that the numerator $2/N|(M+1|\hat{M}_{st}^x|M)|^2$ diverges as

$$\frac{2}{N}|(M+1|\hat{M}_{st}^x|M)|^2 \sim N^\sigma \quad (N \rightarrow \infty), \quad (4-19)$$

with $m = M/N$ fixed. Plots of $\ln [2/N|(M+1|\hat{M}_{st}^x|M)|^2]$ versus $\ln N$ for $m=0, 1/4, 1/2$, and $3/4$ are shown in Fig. 4-2. They look linear for $m \neq 0$, which suggests that (4-19) is valid and χ_{st}^{xx} diverges for $H_{c1} < H < H_{c2}$. In order to consider the size-dependence of χ_{st}^{xx} , we define $\bar{\chi}_{st}^{xx}$ as the value of $\tilde{\chi}_{st}^{xx}$ at $H = (H_M + H_{M+1})/2$ and take $\bar{\chi}_{st}^{xx}$ as an approximation of χ_{st}^{xx} for $m = M/N$. We have checked the form

$$\bar{\chi}_{st}^{xx} \sim N^\omega \quad (N \rightarrow \infty), \quad (4-20)$$

with fixed $m = M/N = 1/4, 1/2$, and $3/4$ respectively, up to $N = 16$. The values of ω , which are estimated by applying (4-20) to $\bar{\chi}_{st}^{xx}$, are shown in Table 4-1, where we use the value derived from the largest- and second-largest-size data of $\bar{\chi}_{st}^{xx}$, and estimate the error based on the difference from the value derived from the second- and

third-largest-size ones. In addition, in order to check the scaling relation

$$\omega = 2 - \eta, \quad (4-21)$$

we extrapolate the spin correlation exponent η calculated by eq. (3-10) linearly to $1/N^2$ for $m = 1/4, 1/2,$ and $3/4,$ and show the results in Table 4-1. The relation (4-21) is satisfied within the errors. The relation (4-21) is of two-dimensional classical systems, and is also derived from the conformal invariance⁸. Therefore, this analysis is consistent with the result in chapter 3.

Now we determine the asymptotic form of χ_{st}^{xx} for $H \sim H_{c1}$ ($H < H_{c1}$). Here we also define $\tilde{\chi}_{st}^{xx}$ as

$$\tilde{\chi}_{st}^{xx} \equiv \frac{2}{N} |\langle 1 | \hat{M}_{st}^x | 0 \rangle|^2 \left(\frac{1}{H_{c1} - H} + \frac{1}{H_{c1} + H} \right), \quad (4-22)$$

where we use $\langle -1 | \hat{M}_{st}^x | 0 \rangle = \langle 1 | \hat{M}_{st}^x | 0 \rangle$. According to our numerical check up to $N = 14,$ $\tilde{\chi}_{st}^{xx}$ is also a good approximation for $0 \leq H < H_{c1},$ and the difference between $\tilde{\chi}_{st}^{xx}$ and χ_{st}^{xx} decreases as H approaches $H_{c1}.$ It suggests that only the first term of (4-22) contributes to the divergence of χ_{st}^{xx} at $H_{c1}.$ In order to make sure of it, we consider the second lowest-energy state which has a non-zero matrix element of \hat{M}_{st}^x with $|0\rangle.$ This state must be in the subspace where $\sum_j S_j^z = 1$ and $k = \pi.$ We define $|1\rangle_2$ as the second lowest-energy state in the subspace and $E_2(N, 1)$ as its energy

for an N -site system. We calculate $E_2(N, 1)$ up to $N = 16$ and plot $E_2(N, 1) - E(N, 1)$ versus $1/N$ in Fig. 4-3. It suggests that there is a gap between $|1\rangle_2$ and $|1\rangle$ even at the thermodynamic limit. The estimated value of this gap is $E_2(N, 1) - E(N, 1) \rightarrow 0.563 \pm 0.001$ ($N \rightarrow \infty$). Therefore we conclude that the asymptotic behavior of χ_{st}^{xx} for $H \sim H_{c1}$ ($H < H_{c1}$) is determined only by the first term of (4-22), because no other term of (4-13) diverges at H_{c1} . Since χ_{st}^{xx} is finite at $H = 0$, the factor $2/N |\langle 1 | \hat{M}_{st}^x | 0 \rangle|^2$ is finite at the thermodynamic limit. Thus we use Shanks' transformation⁹ given by eq. (2-8) to estimate the value of $2/N |\langle 1 | \hat{M}_{st}^x | 0 \rangle|^2$ at the thermodynamic limit. The result is shown in Table 4-2, where we use the data of $2/N |\langle 1 | \hat{M}_{st}^x | 0 \rangle|^2$ for $N = 6, 8, 10, 12$, and 14 , and apply the transformation twice. We did not use the value for $N = 16$ because it leads to misconvergence on the second application of the transformation due to a finite-size effect or a round off. Such a misconvergence sometimes occurs in quantum systems¹⁰. The result of the second transformation in Table 4-2 gives the best estimation we can get, and we determine the error by the difference from the farthest result among the three of the first application of Shanks' transformation. Thus we determine the form of the divergence at H_{c1} as

$$\chi_{st}^{xx} \sim (3.86 \pm 0.06) \frac{1}{H_{c1} - H} \quad (H < H_{c1}), \quad (4-23)$$

at the thermodynamic limit.

Then we give the behavior of χ_{st}^{xx} for the one-dimensional system at the thermodynamic limit as a solid curve in Fig.4-1. The asymptotic forms for $H \sim H_{c1} (H < H_{c1})$ and $H \sim H_{c2} (H > H_{c2})$ are given by (4-23) and (4-16) respectively, and always diverges between H_{c1} and H_{c2} .

§4. 3 Consistency with Experiment

At last we return to the quasi-one-dimensional problem. Treating interchain interactions (4-1) as a mean field, the critical value J_c is given by (4-9). Therefore, within this approximation, we conclude that however small J is, Néel order exists in xy -plane between H_{c1} and H_{c2} , because χ_{st}^{xx} of the one-dimensional system diverges for $H_{c1} < H < H_{c2}$. This order is canted Néel order because finite magnetization exists along z -axis here. Thus, if a measurement is done at sufficiently low temperature, the canted Néel order can be found for $H_{c1} < H < H_{c2}$. In particular a strong signal could be obtained at $m \sim 1/3$, because the transverse spin correlation is strongest there in one-dimensional case. In fact the canted Néel order was observed in the NMR experiment¹¹, but it was reported that the order existed even at $0 < H < H_{c1}$ and its amplitude varied continuously even near H_{c1} . We think that a certain anomalous behavior would be found at H_{c1} if the experiment is done at lower temperature.

References

- ¹ J. P. Renard, M. Verdagner, L. P. Regnault, W. A. C. Erkelens, J. Rossat-Mignod, and W. G. Stirling, *Europhys. Lett.* **3**, 945 (1987).
- ² J. P. Renard, M. Verdagner, L. P. Regnault, W. A. C. Erkelens, J. Rossat-Mignod, J. Ribas, W. G. Stirling, and C. Vettier, *J. Appl. Phys.* **63**, 3538 (1988).
- ³ T. Sakai and M. Takahashi, *Phys. Rev.* **B43**, 13383 (1991).
- ⁴ D. J. Scalapino, Y. Imry, and P. Pincus, *Phys. Rev.* **B11**, 2042 (1975).
- ⁵ T. Sakai and M. Takahashi, *J. Phys. Soc. Jpn.* **58**, 3131 (1989).
- ⁶ T. Sakai and M. Takahashi, *Phys. Rev.* **B42**, 4537 (1990).
- ⁷ R. Kubo, *J. Phys. Soc. Jpn.* **12**, 570 (1957).
- ⁸ J. L. Cardy, in *Phase Transitions and Critical Phenomena*, edited by C. Domb and D. L. Lebowitz (Academic, London, 1987), Vol. 11, Chap. 2, p. 55.
- ⁹ D. Shanks, *J. Math. Phys.* **34**, 1 (1955).
- ¹⁰ T. Sakai and M. Takahashi, *Phys. Rev.* **B42**, 1090 (1990).
- ¹¹ M. Chiba, Y. Ajiro, H. Kikuchi, T. Kubo, and T. Morimoto, *Phys. Rev.* **B44**, 2838 (1991).

Table.4-1 : Exponent η extrapolated linearly to $1/N^2$ from the results of eq. (3 - 10) and exponent ω estimated by eq. (4 - 18), for $m = 1/4, 1/2$, and $3/4$. The scaling relation $\omega = 2 - \eta$ is satisfied within the errors.

m	$m = 1/4$	$m = 1/2$	$m = 3/4$
η	0.348 ± 0.005	0.349 ± 0.001	0.459 ± 0.001
ω	1.66 ± 0.04	1.65 ± 0.01	1.55 ± 0.01

Table.4-2: Results of the Shank's transformation applied to $2/N|\langle 1|\hat{M}_{st}^x|0\rangle|^2$ twice. The column with three data is the result from the first transformation and the right-hand value is from the second one which is the best value we can get here. The error is estimated by the difference from the farthest result among the three results of the first transformation. Thus we estimate $2/N|\langle 1|\hat{M}_{st}^x|0\rangle|^2 \rightarrow 3.86 \pm 0.06(N \rightarrow \infty)$.

N	$2/N \langle 1 \hat{M}_{st}^x 0\rangle ^2$	<i>once</i>	<i>twice</i>
6	2.457651		
8	2.797896	3.845386	
10	3.054720	3.832626	3.859898
12	3.247799	3.808645	
14	3.391431		

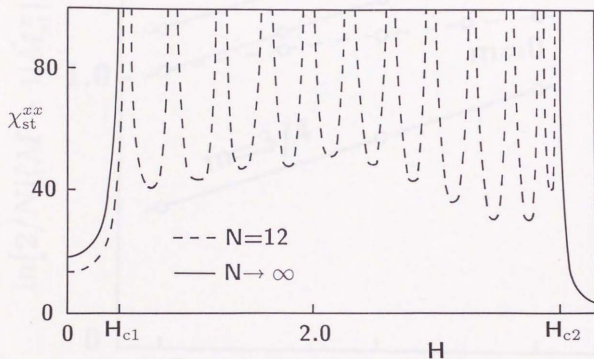


Fig. 4-1. Transverse staggered susceptibility χ_{st}^{xx} at $T = 0$ plotted versus H for $N = 12$ (a dashed curve) and the thermodynamic limit (a solid curve). The latter always diverges between H_{c1} and H_{c2} , and has the asymptotic form $\chi_{st}^{xx} \sim (H_{c1} - H)^{-1}$ at $H \sim H_{c1}$ ($H < H_{c1}$). The form $\chi_{st}^{xx} = (H - H_{c2})^{-1}$ for $H > H_{c2}$ is independent of N .

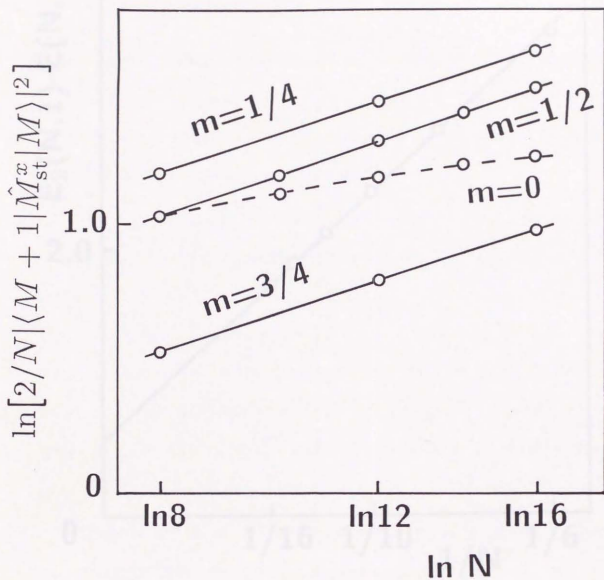


Fig. 4-2. Plots of $\ln[2/N|\langle M + 1|\hat{M}_{st}^x|M\rangle|^2]$ versus $\ln N$ with $m = 0, 1/4, 1/2,$ and $3/4$ fixed respectively. The plots are almost linear for $m \neq 0$ (solid curves), which suggests that the numerator of (4-15) diverges as $2/N|\langle M + 1|\hat{M}_{st}^x|M\rangle|^2 \sim N^\sigma$.

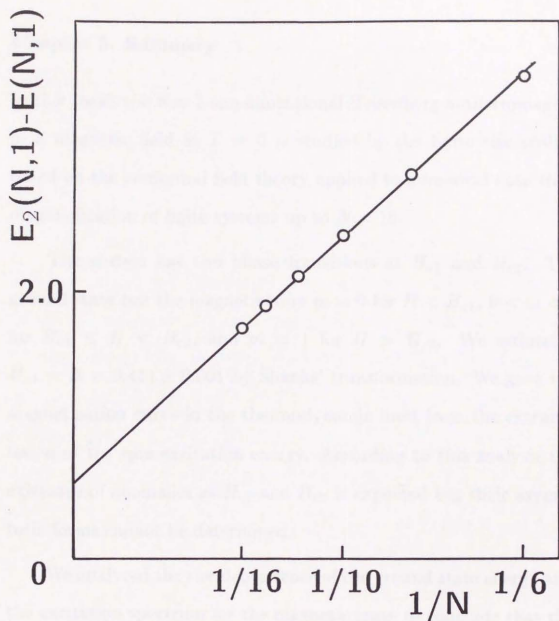


Fig. 4-3. Plot of $E_2(N,1) - E(N,1)$ versus $1/N$. It suggests that a finite gap exists between the lowest- and second lowest-energy states in the subspace where $\sum_j S_j^z = 1$ and $k = \pi$, even at the thermodynamic limit. The estimated gap is 0.563 ± 0.001 . Here we use the same extrapolation in Fig. 2-6.

Chapter 5. Summery

In this thesis the $S = 1$ one-dimensional Heisenberg antiferromagnet in a magnetic field at $T = 0$ is studied by the finite size scaling based on the conformal field theory applied to numerical data from diagonalization of finite systems up to $N = 16$.

The system has two phase transitions at H_{c1} and H_{c2} . The ground state has the magnetization $m = 0$ for $H < H_{c1}$, $0 < m < 1$ for $H_{c1} < H < H_{c2}$, and $m = 1$ for $H > H_{c2}$. We estimated $H_{c1} = \Delta = 0.411 \pm 0.001$ by Shanks' transformation. We gave the magnetization curve in the thermodynamic limit from the extrapolation of the spin-excitation energy. According to this analysis the existence of anomalies at H_{c1} and H_{c2} is expected but their asymptotic forms cannot be determined.

We analyzed the size dependence of the ground state energy and the excitation spectrum for the magnetic state to conclude that the ground state is massless and the system obeys the conformal field theory with $c = 1$ for $0 < m < 1$, and to estimate the exponents η and η^z of spin correlations decaying algebraically. We found that the relation $\eta\eta^z = 1$ is satisfied and the system can be described as the Luttinger liquid. The extrapolation of η and η^z yielded the result that $\eta = 1/2$ and $\eta^z = 2$ in both limits $m \rightarrow 0+$ and $m \rightarrow 1-$, which means that the magnetic excitation can be described as a free fermion

in the limits. Thus we concluded that the anomalous behaviors of the magnetization curve at H_{c1} and H_{c2} have the forms

$$m \simeq (H - H_{c1})^{1/2}, \quad 1 - m \simeq (H_{c2} - H)^{1/2},$$

respectively.

The rotational symmetry in xy -plane is not broken even for $0 < m < 1$ in one dimension. In quasi-one dimension, however, interchain interactions break it and the canted Néel order occurs, within a mean field approximation for interchain interactions. It is consistent with a recent NMR measurement for NENP at low temperature.

Acknowledgements

The author would like to express his sincere gratitude to Professor Minoru Takahashi for his continual guidance and encouragement throughout the course of the present work. He wishes to thank Drs. Hirokazu Tsunetsugu, Miki Yamada and Kiyohide Nomura for valuable discussions. He wishes to acknowledge continual encouragement by Professor Yoshinori Takahashi, Mrs. Kyoko Fujii and Mrs. Akemi Fukui. Many fruitful discussions with all members of the research groups under Professors M. Takahashi, T. Moriya, K. Terakura and M. Imada are also acknowledged.

The numerical calculations were performed by HITAC S-820-80 in the computer center at University of Tokyo, and S-820-80E at HITACHI Kanagawa Works.

